J. Fluid Mech. (1999), *vol.* 379, *pp.* 23–38. Printed in the United Kingdom

Enhancement of three-dimensional instability of free shear layers

By VIVEK SAXENA[1]†, SIDNEY LEIBOVICH[1], AND GAL BERKOOZ[2]

[1] Sibley School of Mechanical and Aerospace Engineering, Cornell University, Ithaca, NY 14853, USA

[2] BEAM Technologies Inc., Ithaca, NY 14850, USA

(Received 20 January 1997 and in revised form 6 August 1998)

Enhancement of the temporal growth rate of inviscid three-dimensional instability waves in free shear layers by deformation of the basic flow is studied. The deformation of a two-dimensional mixing layer is assumed to yield a base flow that remains unidirectional, but has a steady spanwise speed variation in addition to the two-dimensional shear. The computed growth rates for hyperbolic tangent base flow, perturbed this way, show enhanced instability in the sense that the neutral waves of the unperturbed flow exhibit positive growth rates. For each imposed spanwise periodicity, an oblique mode is selected that shows maximum growth rate. The results are consistent with related theoretical studies and with qualitative observations in experiments.

1. Introduction

Enhancement of the instability of free shear layers is often desirable. In reacting flows, such as in a gas turbine combustor, one needs to trigger an early three-dimensional 'mixing transition' of the fuel/air jets to have efficient mixing. Jet exhaust noise abatement would be promoted by reduction of the jet velocity by enhanced jet spreading aided by the instability growth.

The mixing layer has an instability due to an inflection point in the velocity profile. The linear instability manifests itself as an eigenvalue with positive real part, and the eigenfunction corresponding to the most unstable mode is two-dimensional. The two-dimensional flow emerging from this instability subsequently suffers a secondary instability to three-dimensional perturbations. The development of secondary instability has been the subject of a number of analytical and computational investigations, including those of Comte, Lesieur & Lamballais (1992), Corcos & Lin (1984), Pierrehumbert & Widnall (1982), and Moser & Rogers (1993). Once three-dimensional perturbations set in, the mixing is rapid (Moser & Rogers 1993).

Our objective here is to analyse a passive forcing mechanism that will enhance the linearized three-dimensional instability of mixing layers by altering the base flows to make them spanwise-periodic. Rather than reliance on naturally occurring disturbances to initiate cross-stream variation, we contemplate imprinting the basic flow with such a variation, to determine how to enhance the (temporal) instability.

† Present address: Aero/Acoustics/CFD, Mail Stop 163-17, Pratt & Whitney, 400 Main Street, E. Hartford, CT 06108, USA.

Our ultimate goal is to be able to 'design' the basic flow by appropriate manipulation so as to lead to the most rapid breakdown of shear layers.

It is experimentally known (Ahuja & Brown 1989 and Zaman 1993, among others) that passive tabs can alter the stability of shear layers in jets. These tabs mainly generate streamwise vorticity, producing substantial distortions in the flow field – their effect is not that of a small perturbation to the shear flow, but rather in reshaping of it. On the other hand, experiments have been done with indented and corrugated trailing edges of splitter plates (Lasheras & Choi 1988) to study the effect of small spanwise-periodic perturbations to the mean flow. One of their main conclusions was that for large spanwise wavelengths, a wide band of instability waves had comparable growth rates. No quantitative picture of the mean profile or that of growth rates were presented, however. Nygaard & Glezer (1991) presented experimental results for a plane mixing layer forced by a flush-mounted heating mosaic placed near the trailing edge of the splitter plate. They measured the mean profile and observed that a spanwise periodicity is induced by this forcing. The authors suggest that the spanwise periodicity is a result of streamwise vorticity produced by the heating mosaic. However, it is equally likely that the spanwise periodicity is in the vertical vorticity, resulting from deformation of the base flow by the heating elements. We show below that streamwise vorticity can then be generated by the instability of this perturbed mean flow.

Our method of analysis is similar in spirit to that of Kelly (1967), who modelled the generation of the sub-harmonic of the primary two-dimensional instability of the hyperbolic tangent profile, and which has close connections to studies on instability in boundary layers with longitudinal vortex structures (for example, Hall & Horseman 1991 and Goldstein & Wundrow 1995).

The analysis presented here is of the inviscid linearized instability of a unidirectional basic flow† that represents an imposed spanwise-periodic distortion of the classical shear layer (with no longitudinal vorticity). This might be regarded as a generalization of early work by Hocking (1963) on imposed distortions of a vortex sheet, who also found that base flow distortions can lead to enhancement of growth rates. The stability problem for vortex sheets, however, is ill-posed and one is unable to determine finite preferred growth rates, enhanced or otherwise. Consideration of a finite thickness for the shear layer is known to remove such difficulties. The analysis can be carried furthest when the distortion is weak, as measured by a small parameter, δ, defined later. The amplitude A of the linear instability waves is written as

$$\frac{1}{A}\frac{\mathrm{d}A}{\mathrm{d}t} = a_0 + a_1\delta + a_2\delta^2 + \cdots.$$

The coefficients, a_1, a_2 etc., determine the alteration in linear stability characteristics. We evaluate these for neutral modes of the base profile, which corresponds to the case $a_0 = 0$. Wavenumbers corresponding to neutral growth for the base profile are shown to exhibit non-zero growth rates for the modified profile depending on the spanwise-periodic deformation of the flow. Our numerical calculations are carried out for a hyperbolic tangent profile modified by a small-amplitude spanwise-periodic Gaussian perturbation.

† A referee has brought to our attention the report by Wundrow (1996), who has considered a similar problem and presented results for spanwise perturbations of a Blasius boundary layer.

2. Formulation

2.1. *Basic flow*

We work in Cartesian $\boldsymbol{x} = (x_1, x_2, x_3)$ coordinates, with unit vectors $(\boldsymbol{e}_1, \boldsymbol{e}_2, \boldsymbol{e}_3)$. Flows with velocity $U(x_2, x_3)\boldsymbol{e}_1$, are exact solutions of the Euler equations for any $U(x_2, x_3)$. Stability analysis of such a flow leads to a non-separable eigenvalue problem for the Euler equations, linearized about the base flow.

We suppose that the flow downstream of a splitter plate dividing two streams of differing speeds has been shaped by spanwise arrays of heaters, solid protuberances, or other methods to yield a flow with velocity $U(x_2, x_3)\boldsymbol{e}_1$ that is periodic in x_3, and that these devices can be henceforth ignored for the purposes of a temporal stability analysis. There is no loss in generality in adopting a coordinate system that moves with the mean speed of the base flow.

The flow is confined between parallel planes at the dimensionless locations $x_2 = \pm h$. Our principal interest is in the "conventional case" for which $h \to \infty$.

2.2. *Temporal eigenvalue problem*

The evolution of the Laplacian of the velocity field $\boldsymbol{U}$ is obtained by taking the curl of the Navier–Stokes equations twice, yielding

$$\Delta\left[\frac{\partial \boldsymbol{U}}{\partial t} + \boldsymbol{U}\cdot\nabla\boldsymbol{U} - R^{-1}\Delta\boldsymbol{U}\right] = \nabla\left[\nabla\cdot\{\boldsymbol{U}\cdot\nabla\boldsymbol{U}\}\right] \tag{2.1}$$

where ∇ is the three-dimensional Laplacian operator. This equation is exact for the non-dimensionalized form of full Navier–Stokes equations, and any initially solenoidal vector $\boldsymbol{U}$ satisfying this set remains solenoidal. The length and velocity scales are chosen to be L_* (the vorticity half-thickness of the shear layer) and U_* (here taken to be half the speed difference across the mixing layer) respectively. We make these choices of scales, but continue to use same notation for dimensionless variables. We are interested in the inviscid case for which the Reynolds number $R = U_*L_*/\nu$ is infinitely large.

The velocity field is linearized about the unidirectional mean shear profile $U(x_2, x_3)$,

$$\boldsymbol{U} = U(x_2, x_3)\boldsymbol{e}_1 + \boldsymbol{u}(\boldsymbol{x}, t). \tag{2.2}$$

Let

$$\Delta_2 = \Delta - \frac{\partial^2}{\partial x_1^2}$$

be the two-dimensional (x_2, x_3) Laplacian and ∇_2 be the corresponding two-dimensional gradient. Substituting (2.2) into (2.1), setting $R = \infty$, and linearizing gives

$$\Delta\left\{\left(\frac{\partial}{\partial t} + U\frac{\partial}{\partial x_1}\right)\boldsymbol{u} + (\boldsymbol{u}\cdot\nabla_2 U)\,\boldsymbol{e}_1\right\} = 2\frac{\partial}{\partial x_1}\nabla\{\boldsymbol{u}\cdot\nabla_2 U\}, \tag{2.3}$$

where continuity has been used.

The components of equation (2.3) in the plane normal to $\boldsymbol{e}_1$ do not involve the u_1 component. We therefore consider only the pair of equations in this crossplane, and construct u_1 later using continuity. If we denote the two-dimensional vector $(u_2, u_3) = \boldsymbol{v}$, then the components of (2.3) in the (x_2, x_3)-plane may be written compactly as

$$\frac{\partial \Delta\boldsymbol{v}}{\partial t} - \frac{\partial \mathscr{L}(U)\boldsymbol{v}}{\partial x_1} = 0. \tag{2.4}$$

We now suppose that the distortion of the basic flow is weak, as measured by a small parameter δ. In the following, we study the effects of the particular distortion

$$U(x_2, x_3) = U_0(x_2) + 2\delta U_1(x_2)\cos(\beta x_3). \tag{2.5}$$

The linearized operator $\mathscr{L}(U)$ in (2.4) depends on the parameter δ and can be expanded as

$$\mathscr{L}(U) = \boldsymbol{L}_0 + \delta \boldsymbol{L}_1,$$

prompting the corresponding expansion for $\boldsymbol{v}$,

$$\boldsymbol{v} = \boldsymbol{v}^{(0)} + \delta \boldsymbol{v}^{(1)} + \delta^2 \boldsymbol{v}^{(2)} + \cdots.$$

At the lowest order ($O(1)$), we find

$$\frac{\partial \Delta \boldsymbol{v}^{(0)}}{\partial t} - \frac{\partial \boldsymbol{L}_0 \boldsymbol{v}^{(0)}}{\partial x_1} = 0 \tag{2.6}$$

where

$$\boldsymbol{L}_0 = \begin{pmatrix} U_0'' - U_0\Delta & 0 \\ 2U_0'\mathscr{D} & -U_0'' - U_0\Delta - 2U_0'\mathscr{D} \end{pmatrix},$$

where a prime represents the derivative of a function of a single variable with respect to its argument, and where we also introduce $\mathscr{D} = \partial(\cdot)/\partial x_2$.

The problem posed at this order is the usual stability problem for the two-dimensional parallel flow $U_0(x_2)$, leading to the Rayleigh equation.

At $O(\delta)$,

$$\frac{\partial \Delta \boldsymbol{v}^{(1)}}{\partial t} - \frac{\partial \boldsymbol{L}_0 \boldsymbol{v}^{(1)}}{\partial x_1} = \frac{\partial}{\partial x_1}\left[(\mathrm{e}^{\mathrm{i}\beta x_3}\boldsymbol{L}_1 + \mathrm{e}^{-\mathrm{i}\beta x_3}\boldsymbol{L}_1^*)\boldsymbol{v}^{(0)}\right]. \tag{2.7}$$

Here

$$\boldsymbol{L}_1 = \begin{pmatrix} U_1'' - U_1\left[\Delta - \beta^2 + 2\mathrm{i}\beta\dfrac{\partial}{\partial x_3}\right] & 2\mathrm{i}\beta[U_1\mathscr{D} + U_1'] \\ 2U_1'\left[\dfrac{\partial}{\partial x_3} + \mathrm{i}\beta\right] & -U_1'' - U_1\Delta - \beta^2 U_1 - 2U_1'\mathscr{D} \end{pmatrix},$$

and $\boldsymbol{L}_1^*$ is its complex conjugate. In general, the equations at $O(\delta^q)$ are of the form

$$\frac{\partial \Delta \boldsymbol{v}^{(q)}}{\partial t} - \frac{\partial \boldsymbol{L}_0 \boldsymbol{v}^{(q)}}{\partial x_1} = \frac{\partial}{\partial x_1}\left[(\mathrm{e}^{\mathrm{i}\beta x_3}\boldsymbol{L}_1 + \mathrm{e}^{-\mathrm{i}\beta x_3}\boldsymbol{L}_1^*)\boldsymbol{v}^{(q-1)}\right] \tag{2.8}$$

and the problems posed for the $\boldsymbol{v}^{(q)}$ can be solved sequentially. We will need to apply $\boldsymbol{L}_1$ to vectors of normal mode form, so for later reference we note that if $\boldsymbol{f} = \hat{\boldsymbol{f}}(x_2)\mathrm{e}^{\mathrm{i}(\ell x_1 + m x_3)}$ then

$$\boldsymbol{L}_1 \boldsymbol{f} = \mathrm{e}^{\mathrm{i}(\ell x_1 + m x_3)}\hat{\boldsymbol{L}}_1(\ell, m)\hat{\boldsymbol{f}}, \tag{2.9}$$

where

$$\hat{\boldsymbol{L}}_1(\ell, m) = \begin{pmatrix} U_1'' + U_1\left((m+\beta)^2 + \ell^2 - \mathscr{D}^2\right) & 2\mathrm{i}\beta[U_1\mathscr{D} + U_1'] \\ 2\mathrm{i}U_1'[m+\beta] & -U_1'' - U_1\left(\mathscr{D}^2 + \beta^2 - \ell^2 - m^2\right) - 2U_1'\mathscr{D} \end{pmatrix}, \tag{2.10}$$

and $\hat{\boldsymbol{L}}_1^*(\ell, m)$ is obtained by changing the sign of β.

2.3. *Boundary conditions*

A discussion of the boundary conditions and the domain for which (2.8) is to be solved is relevant here to rationalize the present analysis about the neutral mode of the base profile.

Theoretical works on the stability of mixing layers commonly begin by perturbation centred on the neutral modes. When the flow domain is unbounded, and the fluid is treated as inviscid, the flow is unstable. The significance of the analysis about a neutral mode is therefore unclear. This awkward issue is seldom discussed in the literature.

We address this issue by formulating our problem for a mixing layer for which the growth rate of the linearly most unstable mode can be controlled. This can be accomplished by confining the mixing layer between plane walls located at $x_2 = \pm h$, where h is a finite length, leading to a 'ducted mixing layer'.

In this case, even though the necessary criteria of Rayleigh (1880) and Fjørtøft (1950) allow for instability, the inflectional flow is inviscidly stable for sufficiently small h. The maximum growth rate, σ_{max} for any two-dimensional mixing layer profile is a function of h, and marginal stability obtains for a specific value $h = h_*$. Results of calculations for a $\tanh(x_2)$ ducted shear layer are presented in the Appendix.

When the shear layer is placed in a channel of non-dimensional height $2h$, the boundary conditions at $|x_2| = h$ are

$$u_2^{(q)} = 0 = \frac{\partial}{\partial x_2}\left[\left(\frac{\partial}{\partial t} + U_0\frac{\partial}{\partial x_1}\right)u_3^{(q)}\right] \tag{2.11}$$

which comes from $u_2^{(q)} = 0$ together with the momentum equations and their x_2 derivative at the boundary, and the continuity equation.

3. Stability analysis

We begin by exploring the stability characteristics of a ducted shear layer. The results for an unbounded mixing layer will be obtained by letting $h \to \infty$ in the next section.

At the lowest order, the equation for the normal modes of $u_2^{(0)}$ is not coupled to that for $u_3^{(0)}$, and presents the problem for the stability of the flow without x_3 dependence. It is known that the least stable solution for this equation is independent of x_3. Thus $u_2^{(0)}$ is determined by equation (2.6). Adopting a normal form representation and denoting complex conjugation terms by c.c.

$$u_2^{(0)} = \hat{u}_2^{(0)}(x_2)\mathrm{e}^{\mathrm{i}k(x_1-ct)+\mathrm{i}\gamma x_3} + \text{c.c.}$$

where k and γ are streamwise and spanwise wavenumbers, (2.6) reduces to the Rayleigh equation for $\hat{u}_2^{(0)}(x_2)$,

$$\mathscr{D}^2\hat{u}_2^{(0)} - \kappa^2\hat{u}_2^{(0)} - \hat{u}_2^{(0)}\frac{U_0''}{U_0 - c} = 0 \tag{3.1}$$

where $\kappa^2 = k^2 + \gamma^2$ is the magnitude of the wavenumber vector, $\boldsymbol{\kappa} = k\boldsymbol{e}_1 + \gamma\boldsymbol{e}_2$. Since our focus is on temporal stability, we regard k and γ as real, and c as an eigenvalue to be determined.

For a monotonic U_0 with an inflection point, any neutral mode solutions of (3.1) will be regular. We suppose that h is large enough for a neutral mode to exist, with wavenumber κ. The equation for the normal mode form for the spanwise component

$u_3^{(0)}$ is found from (2.6), and leads to an equation analogous to the Rayleigh equation,

$$U_0(\mathscr{D}^2\hat{u}_3^{(0)} - \kappa^2\hat{u}_3^{(0)}) + U_0''\hat{u}_3^{(0)} + 2U_0'\hat{\mathscr{D}}u_3^{(0)} = 2\mathrm{i}\gamma U_0'\hat{u}_2^{(0)}. \tag{3.2}$$

This may be recast for $W^{(0)} = U_0\hat{u}_3^{(0)}$ as

$$\mathscr{D}^2W^{(0)} - \kappa^2W^{(0)} = 2\mathrm{i}\gamma U_0'\hat{u}_2^{(0)} \tag{3.3}$$

with $\mathscr{D}W^{(0)} = 0$ at $x_2 = |h|$.

The solution of (3.3) for non-zero γ is

$$W^{(0)} = -\frac{2\mathrm{i}\gamma}{\kappa\sinh(2\kappa h)}\int_{-h}^{h} R(\eta)G(x_2,\eta)\mathrm{d}\eta, \tag{3.4}$$

where

$$R(x_2) = U_0'\hat{u}_2^{(0)},$$
$$G(x_2,\eta) = \begin{cases} \cosh\kappa(x_2-h)\cosh\kappa(\eta+h), & \eta < x_2 \\ \cosh\kappa(x_2+h)\cosh\kappa(\eta-h), & \eta > x_2. \end{cases}$$

This shows that $\hat{u}_3^{(0)} = W^{(0)}/U_0$ is purely imaginary. It is singular at the critical level $x_2 = y_c = 0$ for $\gamma \neq 0$, whereas $\hat{u}_2^{(0)}$ is smooth everywhere. For plane waves, $\gamma = 0$, and the solution is $W^{(0)} = \mathrm{e}^{-|\kappa|x_2}$, which is now real but $\hat{u}_3^{(0)}$ is still singular at the critical level. This singularity compounds at higher order, and u_2, which is non-singular at lowest order, is singular at higher order since $\hat{u}_3^{(0)}$ appears in the source terms for (2.7). These singularities become increasingly severe at higher orders. The usual way of getting around this is to reintroduce viscosity in a thin layer across y_c (e.g. Maslowe 1986). Alternatively, the critical layer singularity may be resolved by retaining the vestige of time dependence. We will adopt the latter approach to calculate the singular quantities using the standard complex analysis without resorting to the analytically more complicated viscous critical layer theories.

3.1. *The effect of spanwise periodicity*

We assume that by confining the shear layer we are able to control the maximum growth rates of the zeroth-order eigenmodes to near-neutral values. Once these modes have been obtained, our next task is to determine whether the deformation of the base flow has any effect on them.

To this end, we sequentially consider (2.8) with $q = 1, 2, \ldots$. Although the eigenmodes do not interact with each other in our linear analysis, one can think of this problem as a wave-interaction problem, with the perturbation wavy modes interacting with the imposed spanwise-periodic base flow deformation acting as a 'pump wave', so that the problem at $O(\delta^2)$ may be thought of as a three-wave interaction (Craik 1985).

We start with (2.7) with known right-hand side $\hat{v}_i^{(0)}$. A solution is possible if the non-homogeneous terms are orthogonal to the solution of the homogeneous adjoint problem (Ince 1956). We therefore find the solution (denoted by $\boldsymbol{\Phi}$) to the adjoint equation to the steady form of (2.6). We then take the inner product of this adjoint solution with (2.7) and ensure that the right-hand side of the product vanishes.

3.2. *The adjoint equation*

The adjoint operator is defined as $(\boldsymbol{\Phi}, \boldsymbol{L}\boldsymbol{u}) = (\boldsymbol{L}^{ad}\boldsymbol{\Phi}, \boldsymbol{u})$ where $(\boldsymbol{f}, \boldsymbol{g}) = \langle \boldsymbol{f}\cdot\boldsymbol{g}^* \rangle = \int_V \boldsymbol{f}\cdot\boldsymbol{g}^*\mathrm{d}V$ is the inner product of $\boldsymbol{f}$ and $\boldsymbol{g}$ (and the asterisk represents complex conjugation).

The adjoint equations to the steady form of (2.6) are

$$\Delta[U_0\phi] + 2U_0'\frac{\partial\chi}{\partial x_3} - U_0''\phi = 0, \tag{3.5}$$

$$\Delta[U_0\chi] - 2U_0'\mathscr{D}\chi - U_0''\chi = 0, \tag{3.6}$$

where the inner product of $\boldsymbol{\Phi} = (\phi, \chi)$ with the right-hand side of (2.6) vanishes for the following boundary conditions on $\boldsymbol{\Phi}$:

$$\phi = 0 \quad \text{at} \quad x_2 = |h|$$

and

$$\mathscr{D}\left(\chi/U_0\right) = 0 \quad \text{at} \quad x_2 = |h|.$$

With

$$\boldsymbol{\Phi} = \hat{\boldsymbol{\Phi}}(x_2)\mathrm{e}^{\mathrm{i}k'x_1 + \mathrm{i}\gamma' x_3} + \text{c.c.}$$

we have

$$\left.\begin{aligned} \mathscr{D}^2\left(U_0\hat{\phi}\right) - \kappa^2\left(U_0\hat{\phi}\right) - \frac{U_0''}{U_0}\left(U_0\hat{\phi}\right) = -2\mathrm{i}\gamma U_0'\hat{\chi}, \\ U_0\left(\mathscr{D}^2\hat{\chi} - \kappa^2\hat{\chi}\right) = 0. \end{aligned}\right\} \tag{3.7}$$

The first of these equations is an inhomogeneous Rayleigh equation for $[U_0\hat{\phi}]$ forced by the term $-2\mathrm{i}\gamma U_0'\hat{\chi}$. We start with the equation for $\hat{\chi}$. With the exception of special values of the height h and wavenumber κ satisfying either of the two conditions (i) $\tanh(\kappa h) = U_0'(h)/\kappa U_0(h)$ and (ii) $\tanh(\kappa h) = \kappa U_0(h)/U_0'(h)$, there is no smooth non-zero solution. Case (i) leads to $\hat{\chi} = A\cosh(\kappa x_2)$ and Case (ii) to $\hat{\chi} = A\sinh(\kappa x_2)$ for arbitrary constant A. Otherwise, the solution of the adjoint is the generalized function arising from the solution of either $\mathscr{D}^2\hat{\chi} - \kappa^2\hat{\chi} = \delta(x_2)$ or $\hat{\chi} = 0$, so that $[U_0\hat{\phi}]$ satisfies the homogeneous Rayleigh equation. We adopt the principle of least singularity, which implies that $\hat{\chi} = 0$ is the required solution. Since the boundary conditions for $[U_0\hat{\phi}]$ are also the same as those for $\hat{u}_2^{(0)}$, we have $U_0\hat{\phi} = \hat{u}_2^{(0)}$ and $\left(k'^2 + \gamma'^2\right)^{1/2} = \left(k^2 + \gamma^2\right)^{1/2}$. Since $\hat{u}_2^{(0)} \neq 0$ in general, the adjoint $\hat{\phi} = \hat{u}_2^{(0)}/U_0$ is singular at the critical level y_c.

Since the left-hand side of equations (2.8) at all higher orders is the same, the above adjoint solution is valid for the whole set.

3.3. *Analysis at* $O(\delta)$

We now analyse the two-wave interaction involving the steady mean perturbation with the neutral wave of the base profile. The spanwise and streamwise wavenumbers of the latter are such that $\left(k^2 + \gamma^2\right)^{1/2} = \kappa$ where κ is given by the $O(1)$ analysis. Taking the inner product of $\boldsymbol{\Phi}$ with the equation for $v_i^{(1)}$ (2.7), we get

$$\frac{\partial(\boldsymbol{\Phi}, \Delta\boldsymbol{v}^{(1)})}{\partial t} = \left(\boldsymbol{\Phi}, \mathrm{e}^{\mathrm{i}\beta x_3}\frac{\partial \boldsymbol{L}_1\boldsymbol{v}^{(0)}}{\partial x_1}\right) - \frac{\mathrm{d}A}{\mathrm{d}T_1}\left(\boldsymbol{\Phi}, \Delta[\hat{\boldsymbol{v}}^{(0)}\mathrm{e}^{\mathrm{i}\boldsymbol{\kappa}\cdot\boldsymbol{x}}]\right) + \text{c.c.} \tag{3.8}$$

In writing (2.7), A is an amplitude function, and the need for slow time scales has been anticipated, so that the lowest-order solution is

$$\boldsymbol{v}^{(0)} = A(T_1, T_2, \ldots)\hat{\boldsymbol{v}}^{(0)}(x_2)\mathrm{e}^{\mathrm{i}(kx_1 + \gamma x_3)}$$

where the $T_n = \delta^n t$ are slow time scales introduced to suppress the appearance of secular terms in the expansion and the time derivative expands in the usual way in

terms of the fast time t and the slow times T_n. With these expansions, the first term on the right-hand side of (3.8) is found to vanish by periodicity unless $\gamma' = \gamma + \beta$ and $k = k'$, which is not possible for non-zero β since $k^2 + \gamma^2 = k'^2 + \gamma'^2 = \kappa^2$. Therefore, we do not get an amplitude equation at this order unless the mean flow perturbation is spanwise invariant ($\beta = 0$). The solutions for $v_i^{(1)}$, which represent the eigenmode perturbation in response to the base flow perturbation, are determined by

$$\frac{\partial \Delta \boldsymbol{v}^{(1)}}{\partial t} - \frac{\partial \boldsymbol{L}_0 \boldsymbol{v}^{(1)}}{\partial x_1} = \frac{\partial}{\partial x_1}\left[\mathrm{e}^{\mathrm{i}\beta x_3}\boldsymbol{L}_1 \boldsymbol{v}^{(0)}\right] + \text{c.c.} \tag{3.9}$$

The right-hand side of this equation is $\mathrm{i}kA\mathrm{e}^{\mathrm{i}[kx_1+(\gamma+\beta)x_3]}\hat{\boldsymbol{L}}_1\hat{\boldsymbol{v}}^{(0)} + \text{c.c.}$ There is a steady solution for $\boldsymbol{v}^{(1)}$ of the form

$$\boldsymbol{v}^{(1)} = A\hat{\boldsymbol{v}}^{(1)}(x_2)\mathrm{e}^{\mathrm{i}kx_1+\mathrm{i}(\gamma+\beta)x_3} + \text{c.c.}$$

An explicit solution of this equation is found in a subsequent section for the case of $h \to \infty$.

3.4. *Analysis at* $O(\delta^2)$

From a conceptual viewpoint, this stage of analysis is similar to the three-wave interaction analysis with the mean perturbation providing the two steady 'waves' that interact with the neutral wave of the base flow. Now, the equation for $\boldsymbol{v}^{(2)}$, from (2.8), is

$$\frac{\partial \Delta \boldsymbol{v}^{(2)}}{\partial t} - \frac{\partial \boldsymbol{L}_0 \boldsymbol{v}^{(2)}}{\partial x_1} = \frac{\partial}{\partial x_1}\left[(\mathrm{e}^{\mathrm{i}\beta x_3}\boldsymbol{L}_1 + \mathrm{e}^{-\mathrm{i}\beta x_3}\boldsymbol{L}_1^*)\boldsymbol{v}^{(1)}\right] - \frac{\partial \Delta \boldsymbol{v}^{(0)}}{\partial T_2}, \tag{3.10}$$

where $T_2 = \delta^2 t$. Now, consider the right-hand side of the equation for $u_i^{(2)}$, keeping in mind that $u_i^{(1)} = A\hat{u}_i^{(1)}\mathrm{e}^{\mathrm{i}kx_1+\mathrm{i}(\beta+\gamma)x_3}$. The terms on the right-hand side of (3.10) that involve the streamwise derivative ($\partial/\partial x_1$) are

$$\begin{aligned}&\mathrm{i}kA\mathrm{e}^{\mathrm{i}\kappa\cdot\boldsymbol{X}}\left[\mathrm{e}^{2\mathrm{i}\beta x_3}\hat{\boldsymbol{L}}_1(k,\gamma)\hat{\boldsymbol{v}}^{(1)} + \hat{\boldsymbol{L}}_1^*(k,\gamma)\hat{\boldsymbol{v}}^{(1)}\right]\\ &-\mathrm{i}kA^*\mathrm{e}^{-\mathrm{i}\kappa\cdot\boldsymbol{X}}\left[\mathrm{e}^{-2\mathrm{i}\beta x_3}\hat{\boldsymbol{L}}_1^*(-k,-\gamma)\hat{\boldsymbol{v}}^{(1)*} + \hat{\boldsymbol{L}}_1(-k,-\gamma)\hat{\boldsymbol{v}}^{(1)*}\right].\end{aligned}$$

Taking the inner product of (3.10) with the solution of the adjoint problem ($\boldsymbol{\Phi} = \hat{\boldsymbol{\Phi}}(x_2)\mathrm{e}^{(\mathrm{i}k'x_1+\mathrm{i}\gamma'x_3)}$), and requiring the right-hand side to vanish, yields the condition

$$\frac{\mathrm{d}A^*}{\mathrm{d}T_2}\langle\hat{\boldsymbol{\Phi}}\cdot(\mathscr{D}^2-\kappa^2)\hat{\boldsymbol{v}}^{(0)*}\rangle = -\mathrm{i}kA^*\langle\hat{\boldsymbol{\Phi}}\cdot[\hat{\boldsymbol{L}}_1^*(k,\gamma)\hat{\boldsymbol{v}}^{(1)}]^*\rangle \tag{3.11}$$

whose complex conjugate is

$$\frac{\mathrm{d}A}{\mathrm{d}T_2}\langle\hat{\boldsymbol{\Phi}}^*\cdot(\mathscr{D}^2-\kappa^2)\hat{\boldsymbol{v}}^{(0)}\rangle = -\mathrm{i}kA\langle\hat{\boldsymbol{\Phi}}^*\cdot[\hat{\boldsymbol{L}}_1^*(k,\gamma)\hat{\boldsymbol{v}}^{(1)}]\rangle.$$

Recalling that $\boldsymbol{\Phi} = (\phi, 0)$, the condition (3.11), that ensures non-secularity of the solution, becomes

$$\frac{\mathrm{d}A}{\mathrm{d}T_2}\int_{-h}^{h}\hat{\boldsymbol{\Phi}}^*\cdot(\mathscr{D}^2-\kappa^2)\hat{\boldsymbol{v}}^{(0)}\mathrm{d}x_2 = \mathrm{i}kA\int_{-h}^{h}\hat{\boldsymbol{\Phi}}^*\cdot[\{\mathscr{D}^2U_1+U_1(\kappa^2-\mathscr{D}^2)\}u_2^{(1)} - 2\mathrm{i}\beta\mathscr{D}U_1u_3^{(1)}]\mathrm{d}x_2.$$

Therefore,

$$\frac{1}{A}\frac{\mathrm{d}A}{\mathrm{d}T_2} = \frac{\mathrm{i}k\displaystyle\int_{-h}^{h}\hat{\phi}^*[\{\mathscr{D}^2U_1 + U_1(\kappa^2-\mathscr{D}^2)\}u_2^{(1)} - 2\mathrm{i}\beta\mathscr{D}(U_1u_3^{(1)})]\mathrm{d}x_2}{\displaystyle\int_{-h}^{h}(|\hat{u}_2^{(0)}|^2\mathscr{D}^2U_0)/U_0^2\,\mathrm{d}x_2}, \tag{3.12}$$

where the denominator is simplified using (3.1). The amplitude equation will show an enhanced growth rate if (3.12) has a positive real part. It would now be possible to fix β and formulate a variational problem to maximize (3.12) to determine an optimum shape of $U_1(x_2)$ or, conversely, to fix the shape of mean flow perturbations and find the value of β which gives the maximum linear growth rate.

4. Calculations for the hyperbolic tangent profile

The most common case of a shear profile with an inflection point, representing two streams of different speeds meeting downstream of a splitter plate, is the hyperbolic tangent profile with $h \to \infty$. The temporal instability curve of such a profile was first obtained by Michalke (1964). Our aim here is to show that a neutral wave of $\tanh x_2$ profile for $h = \infty$ can be destabilized when the basic flow is deformed appropriately. Here we choose base flow deformation amplitude variation in (2.5) to be

$$U_1(x_2) = \mathrm{e}^{-x_2^2/s}. \tag{4.1}$$

Note that a negative value of δ in (2.5) implies perturbation due to periodic wakes shed by, for example, a periodic array of tabs whose size scales with the parameter s and which cause a maximum velocity defect of magnitude δ that occurs at the critical level of the base flow. A positive value of δ will correspond to an array of jets with similar interpretations for the parameters.

Before evaluating the effect of the mean perturbation, we shall report the solution of the three-dimensional Rayleigh's equations (3.1) and (3.2). The neutral wave has $\kappa = 1$ and the eigenfunctions are given by

$$\hat{u}_2^{(0)} = \operatorname{sech}\, x_2, \quad \hat{u}_3^{(0)} = \mathrm{i}\gamma\,(\sinh x_2)^{-1}.$$

The solution to the adjoint equations (3.7) have Fourier components:

$$\hat{\phi} = (\sinh x_2)^{-1}, \quad \hat{\chi} = 0.$$

At $O(\delta)$, the governing equations, after some manipulation, may be written as

$$\left\{U_0(\mathscr{D}^2-\alpha^2) - \mathscr{D}^2U_0\right\}\hat{u}_2^{(1)} = 2\mathrm{i}\beta\mathscr{D}(U_1\hat{u}_3^{(0)}) + \left\{\mathscr{D}^2U_1 + U_1(\alpha^2-\mathscr{D}^2)\right\}\hat{u}_2^{(0)}, \tag{4.2}$$

$$\begin{aligned}\left\{U_0(\mathscr{D}^2-\alpha^2) + 2(\mathscr{D}U_0)\mathscr{D} + \mathscr{D}^2U_0\right\}\hat{u}_3^{(1)} &= 2\mathrm{i}(\gamma+\beta)\{(\mathscr{D}U_0)\hat{u}_2^{(1)} + (\mathscr{D}U_1)\hat{u}_2^{(0)}\}\\ &\quad - \left\{\mathscr{D}^2U_1 + U_1\left(\beta^2+\mathscr{D}^2-\kappa^2\right) + 2(\mathscr{D}U_1)\mathscr{D}\right\}u_3^{(0)},\end{aligned} \tag{4.3}$$

where $\alpha^2 = k^2 + (\gamma+\beta)^2$. The differential operators in (4.2) and (4.3) have a regular singular point at the critical level $x_2 = 0$, and the forcing on the right-hand sides involves terms known from $O(1)$ analysis. Clearly, $\hat{u}_2^{(1)}$ may be taken to be purely real and $\hat{u}_3^{(1)}$ purely imaginary for $\gamma \neq 0$. The spanwise component is more singular than the vertical component, the latter having the same singularity as the spanwise component at the previous order. The solutions were computed using a value of the parameter $s = 0.06$, which our subsequent considerations indicate is suitable.

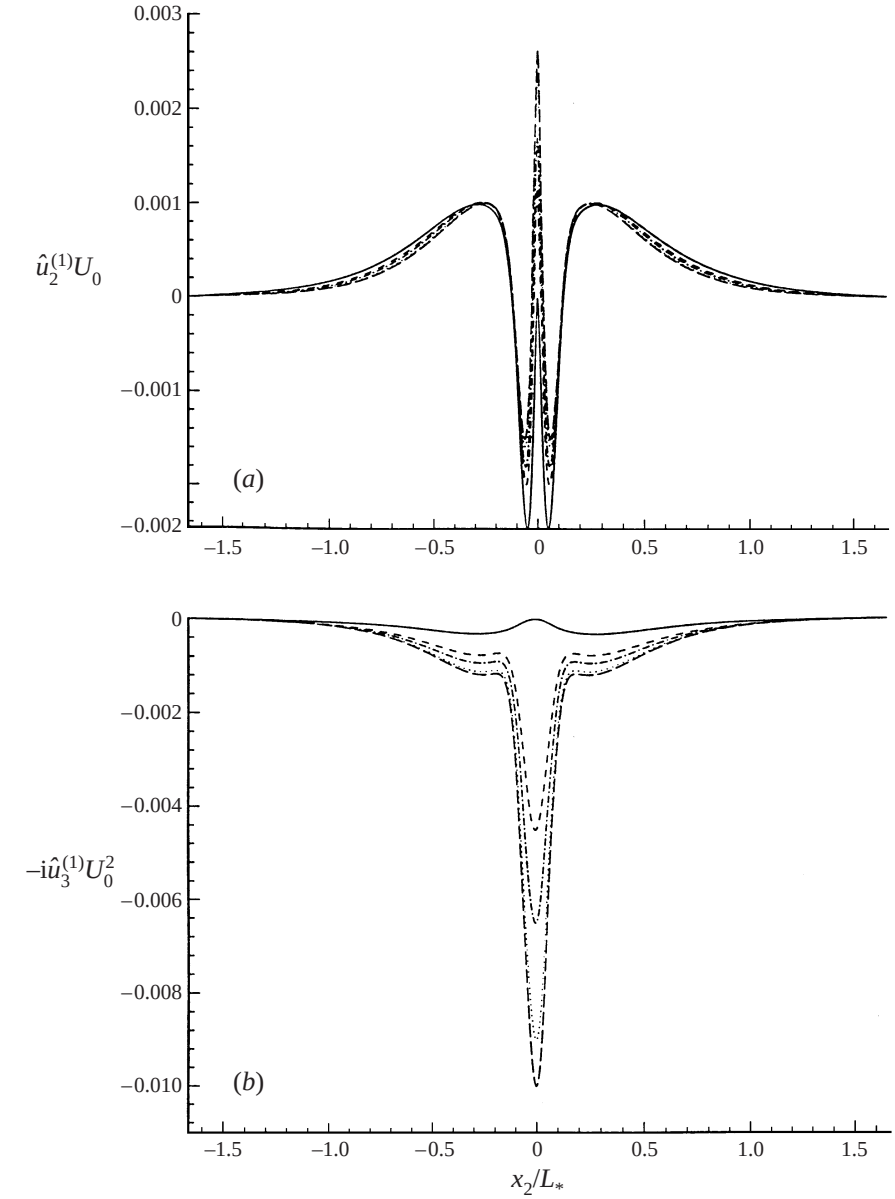

FIGURE 1. Fourier components of (*a*) the normal and (*b*) spanwise amplitude functions resulting from $O(\delta)$ analysis (i.e. solutions of equations (4.2) and (4.3)). The functions have been regularized by multiplying them with appropriate powers of U_0. Here $\beta L_* = 0.75$, and $\gamma L_* = 0$ (2-D mode); - - - - -, $\gamma L_* = 0.003$; ——, $\gamma L_* = 1.35$; · · · · · ·, $\gamma L_* = 1.95$; ——, $\gamma L_* = 2.70$.

Define the wave obliqueness to be $\theta = \tan^{-1}(\gamma/k)$, the angle between the wavenumber vector of the perturbation and the direction (x_1) of the basic flow. The solutions of (4.2) and (4.3) ('regularized' by multiplying with an appropriate power of U_0) are plotted in figures 1 and 2 for two different values of imposed spanwise periodicity. For $\beta L_* = 0.75$, the vertical component of the oblique mode is shown in figure 1(*a*) for various values of the spanwise wavenumber γ. The shapes of this mode for different values of γ vary only slightly across the width of the shear layer, and exhibit

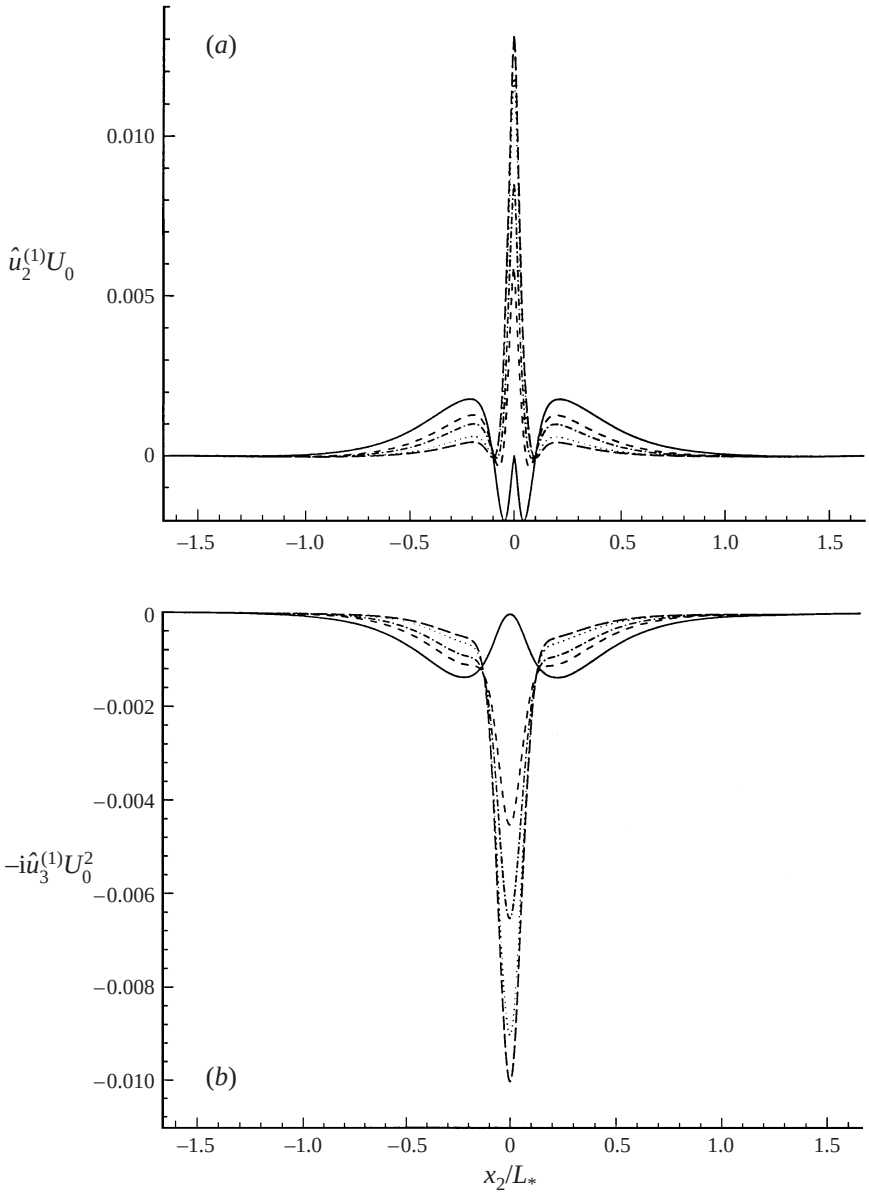

FIGURE 2 (a, b). Same as figure 1 but for $\beta L_* = 7.5$.

behaviour similar to the plane-wave mode shown by the solid line. The spanwise mode, shown in figure 1(b), is more sensitive to the obliqueness angle, and the negative peak value arising in this mode increases monotonically with increasing spanwise wavenumber. Note that streamwise vorticity $\omega_1 = [\mathscr{D}\hat{u}_3 - \mathrm{i}\gamma\hat{u}_2]\,\mathrm{e}^{\mathrm{i}(kx_1+\gamma x_3-ct)}$ has been generated although the imposed vorticity had no streamwise component.

In contrast to the case resulting for $\beta L_* = 0.75$, for $\beta L_* = 7.5$, both the vertical and spanwise components are sensitive to three-dimensional effects, as may be seen in figure (2a, b). While the two-dimensional mode has the same shape and similar magnitude across the width as in $\beta L_* = 0.75$ case, the three-dimensional modes show an order of magnitude larger values at the critical level. There is little difference

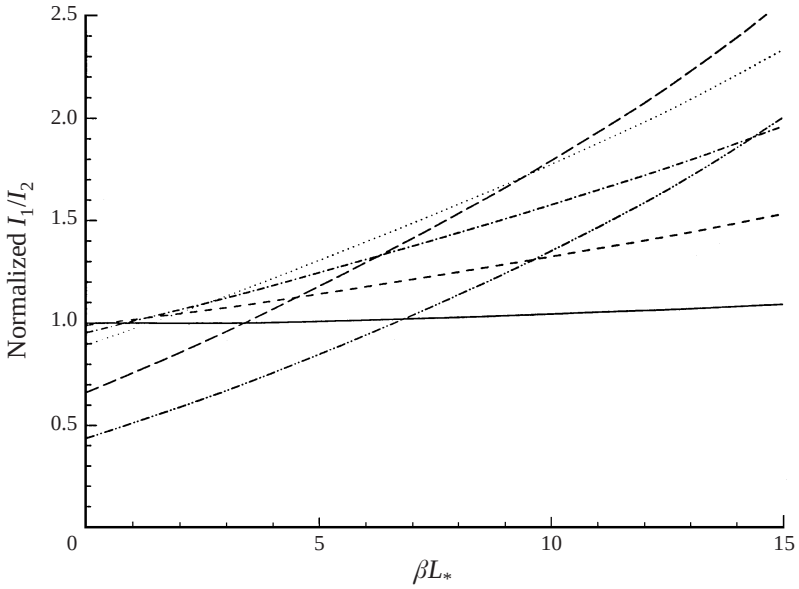

FIGURE 3. Growth rate enhancements (I_1/I_2; normalized by its value when $\gamma \to 0$ and $\beta \to 0$) plotted against imposed spanwise periodicity (β) for different spanwise wavenumbers or oblique modes: $\gamma L_* = 0$ (2-D mode); - - - - - , $\gamma L_* = 0.003$; —·—·—, $\gamma L_* = 1.35$; · · · · · · , $\gamma L_* = 1.95$; —— , $\gamma L_* = 2.70$; —··—··—, $\gamma L_* = 3.00$.

in the behaviour near $x_2 = 0$ in figures 1(b) and 2(b), which respectively give the shape of the spanwise mode for $\beta L_* = 0.75$ and $\beta L_* = 7.5$. Although results for other β values are not included here, as the imposed spanwise wavenumber increases the vertical component grows, but the spanwise component remains unaltered near $x_2 = 0$. Consequently, the changes in the streamwise and normal vorticity at the critical level, that occur as βL_* increases, will not be due to the spanwise perturbation component arising from the instability.

We now have the quantities needed to evaluate the integrals (3.12). The worst singularity in the kernel of I_1 is a pole of order four. We integrate along a contour in the complex-x_2 plane that lies below the singularity. Enhanced instability results when the real part of I_1/I_2 is positive. The results of growth rates are presented in figures 3 and 4 for various values of β and γ. The growth rate in these figures is normalized by its value for the plane waves ($\gamma = 0$) for the particular case when there is no periodicity in the imposed perturbation (i.e. $\beta = 0$). Figure 3 suggests that the plane waves show no appreciable change in the growth rates for the range of β values plotted. The oblique waves, on the other hand, have monotonically increasing growth rates as β increases. At $\beta = 0$, the inviscid version of Squire's theorem holds, and the two-dimensional mode is the most amplified one. Away from this point, the mean flow is no longer two-dimensional and the theorem does not hold, and higher growth rates are found here for at least some of the three-dimensional modes. To each oblique mode, it is possible to assign a $\beta = \beta_c$ above which it shows enhanced instability. A wide range of oblique modes exhibit this behaviour for relatively small values of β. At large β values (the meaning of 'large' is not determined here since the present study is linear in the instability wave magnitude), the growth rates will be modified by diffusive and nonlinear effects that have been ignored here.

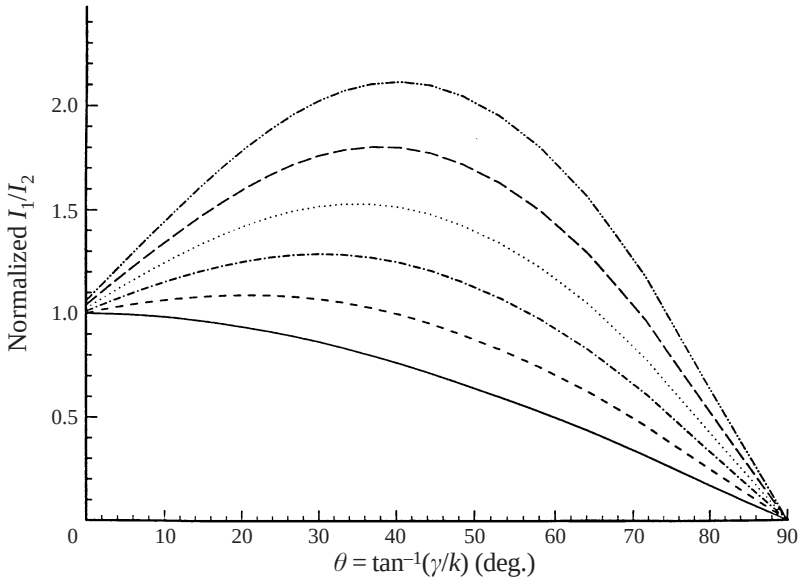

FIGURE 4. Growth rate enhancements (I_1/I_2; normalized by its value when $\gamma \to 0$ and $\beta \to 0$) plotted against instability-wave obliqueness angle ($\theta = \tan^{-1}(\gamma/k)$) from the streamwise direction for different spanwise periodicities (β values): $\beta L_* = 0$ (2-D shear layer); - - - - -, $\beta L_* = 2.4$; —·—·—, $\beta L_* = 4.8$; · · · · · · , $\beta L_* = 7.2$; ——, $\beta L_* = 9.6$; —··—··—, $\beta L_* = 12.0$.

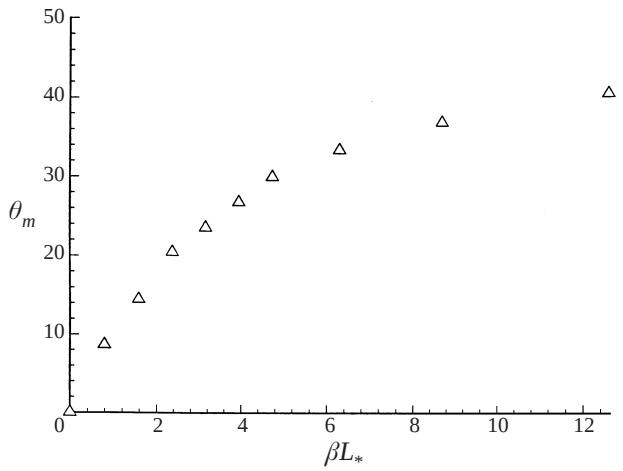

FIGURE 5. Most amplified modes, $\theta_m = \tan^{-1}(\gamma/k)$ corresponding to maximum value of (I_1/I_2) for each β.

Figure 4 plots the same growth rate results against spanwise wavenumber γ, emphasizing the obliqueness effects. There is no preferred mode for sufficiently small β, in qualitative agreement with the experimental findings of Lasheras & Choi (1988). At larger values of β, there is clearly a preferred mode. Figure 5 plots the values of γ for the most amplified mode for each β. It is noted that, in the absence of viscous and nonlinear effects, the wavenumber γ of the most amplified mode tends to asymptote for large values of β.

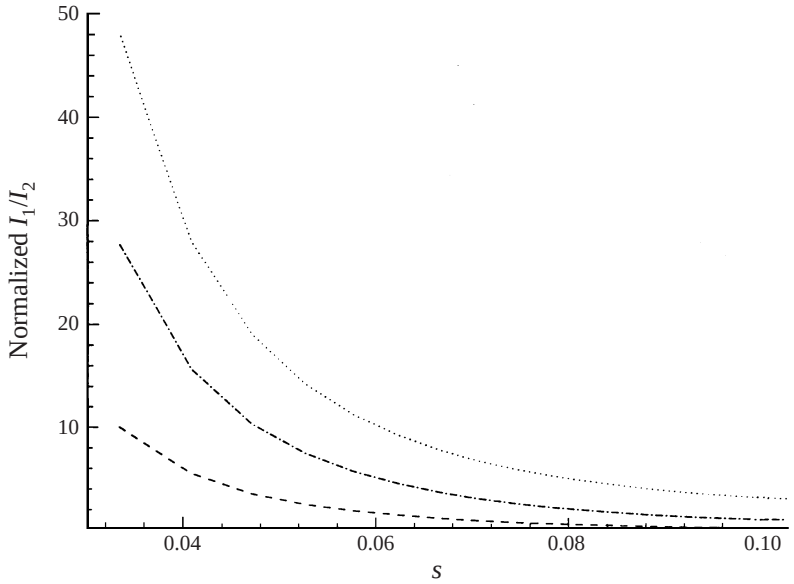

FIGURE 6. Growth rate enhancement (normalized I_1/I_2) variation with the vertical size parameter of the mean flow deformation (see equation (4.1)). - - - - -, $\beta L_* = 4.0$; —·—·—, $\beta L_* = 8.0$; ·····, $\beta L_* = 12.0$.

The vertical length scale of the spanwise base flow deformation is determined by the parameter s. Figure 6 plots the growth rate for various values of β, maximized over γ in each case, as a function of s. The choice of s anticipates that the growth rate enhancement scales with the gradient of the basic flow, and there the deformation from a two-dimensional shear is effected in a vertical length of $O(s^{1/2})$. An interesting feature of this plot is that the growth rate asymptotes for large s values. The limit of large s and large spacing (small β) corresponds to having imposed no deformation at all, i.e. no enhanced growth. The plot also shows that smaller values of s have exponentially large returns. However, viscous effects ignored in the analysis limit how small s can be. The value of s selected in this paper was 0.06, based on considerations to be given below. Note that the magnitude δ and scale s of the base flow deformation are independent parameters. For example, if one thinks of the base flow deformation as being created by suction or blowing, δ measures the level of suction or blowing applied by slotted orifices with vertical extent measured by s.

Ignoring the diffusive terms, expected to be due to turbulent fluctuations, in the stability equations imposes constraints on the applicability of the analysis. The dimensionless eddy diffusivity in a turbulent flow is of order $u'\ell/VL_*$, where u' is the r.m.s. speed and ℓ is the integral length scale. Consequently, diffusive effects will contribute terms of order $(u'\ell/VL_*)(\beta^2 L_*^2)$. This parameter should be neglegibly small for the present analysis to be valid. This will be the case when $\beta L_* \ll (VL_*/u'\ell)^{1/2}$. For example, if the integral length scale of turbulence is 20% of the shear layer half-thickness and turbulence intensity is typically 2%, then there is a high-wavenumber viscous cutoff for βL_* greater than about 16. Consequently, the spanwise placement of the flow manipulators should not be any closer than about 20% of the shear layer thickness. A similar consideration results in the constraint that s should not be much smaller than $L_*^2/125$. This corresponds to $s > 0.06$ for $L_* = 3$ (in figure 6).

5. Discussion

The analysis indicates that it is possible to modify the growth rate of the neutral modes of an inflectional base flow by adding a small, steady, spanwise-periodic, deformation having only a streamwise component. This kind of base flow modification does not involve adding streamwise vorticity to the flow, but rather introduces vorticity components, ω_2 and ω_3, normal to the direction of the base flow. In the unperturbed base flow, there is no net vortex line deformation. Rotation of the ω_2 vorticity component by the shear $\partial U/\partial x_2$ is nullified by a rotation of the spanwise vorticity component ω_3 by the spanwise shear $\partial U/\partial x_3$. This balance is undone when the base flow is perturbed, and streamwise vorticity is generated due to the interaction between the neutral wave of the base profile and the imposed spanwise deformation of the base flow.

Although we have demonstrated enhanced instability by a perturbation analysis for weak $O(\delta)$ spanwise variations of the base flow, leading to an increase in growth rate of $O(\delta^2)$, we believe it virtually certain that enhanced instability will persist to $O(1)$ spanwise variations of the base flow. A Floquet analysis is required for such cases, which permits the mean flow deformation to be arbitrarily large, and of arbitrary spanwise variation, in contrast to the sinusoidal variation required in the present analysis. This allows the consideration of more localized distortions. We anticipate that the growth rate enhancement can be substantial, and we hope to present those results in a follow-up paper.

The numerical calculations in this paper were carried out for the case of a hyperbolic tangent profile deformed by spanwise-periodic Gaussian profiles concentrated on the critical level of the base flow. We find positive growth rates for the neutral modes of the original flow above a particular imposed wavenumber β. Oblique and plane waves have qualitatively different behaviours as β increases, in that the two-dimensional waves remain largely unaffected as β increases but the three-dimensional waves show enhanced growth rates. Experimental observations by Lasheras & Choi (1988) in the limit of large base flow deformation wavelength (small β) show no preferred mode of amplified disturbances, which is consistent with our results. The estimates in the previous section suggest that it should be possible to realize the enhancement in practice.

We have shown that above a certain value of β a preferred oblique mode with maximum growth rate exists at each imposed periodicity. However, the β values at which the most amplified mode becomes independent of β are quite high. It is unlikely that such high imposed wavenumbers are realizable in practice without considering the diffusive and nonlinear effects. Therefore, there is probably no universally preferred mode for the present situation. Each initial condition determines which oblique mode will be most amplified.

This research was supported through a Phase 2 NASA-SBIR, contract no. NAS1-20408, monitored by Dr Jack Seiner. We gratefully acknowledge Dr Seiner for introducing us to the problem and for his many contributions.

Appendix. The neutrally stable ducted shear layer

For finite height of unperturbed hyperbolic shear layer, the problem for $\hat{u}_2^{(0)}$ must be solved numerically. For the neutral case, this reduces to

$$\mathscr{D}^2\hat{u}_2^{(0)} - \kappa^2\hat{u}_2^{(0)} - \hat{u}_2^{(0)}\frac{\mathscr{D}^2U^{(0)}}{U^{(0)}} = 0 \qquad \text{(A 1)}$$

with the following boundary conditions:

$$\hat{u}_2^{(0)}(-h) = 0 = \hat{u}_2^{(0)}(h).$$

Since $-\mathscr{D}^2 U^{(0)}/U^{(0)} = 2\,\mathrm{sech}^2 x_2$ in our case and the problem is a standard Sturm–Liouville eigenvalue problem (with eigenvalue κ^2), we know that a solution will not exist for a positive eigenvalue if

$$\pi^2/(2h_*)^2 > 2 \quad \text{or} \quad h_* < \pi/2\sqrt{2} = 1.12.$$

Rayleigh's equation for neutral modes was also solved numerically for different values of h. The effect of confinement of the shear layer is to reduce the growth rates, most notably at low wavenumbers as one would expect. It was found that as the thickness of the shear layer was reduced, the typical wavenumbers of the band of most amplified waves increased and then gradually became smaller – an intriguing result. No instability could be found for κ^2 below $h_* = 1.15$. This is consistent with (in fact, quite close to) the above lower bound of 1.12.

REFERENCES

Ahuja, K. K. & Brown, W. H. 1989 Shear layer control by mechanical tabs. *AIAA Paper* 89-0994.

Comte, P., Lesieur, M. & Lamballais, E. 1992 Large- and small-scale stirring of vorticity and a passive scalar in a 3-D temporal mixing layer *Phys. Fluids* A **4**, 2761–2778.

Corcos, G. M. & Lin, S. J. 1984 The mixing layer: deterministic models of a turbulent flow. Part 2. The origin of the three dimensional motion. *J. Fluid Mech.* **139**, 67–95.

Craik, A. D. D. 1985 *Wave Interactions and Fluid Flows.* Cambridge University Press.

Fjørtøft, R. 1950 Application of integral theorems in deriving criteria for stability of laminar flows and for the baroclinic circular vortex. *Geofys. publ. Oslo* **17** No. 6, 1–52.

Goldstein, M. E. & Wundrow, D. W. 1995 Interaction of oblique instability waves with weak streamwise vortices *J. Fluid Mech.* **284**, 377–407.

Hall, P. & Horseman, N. J. 1991 The linear inviscid secondary instability of longitudinal vortex structures in boundary layers. *J. Fluid Mech.* **232**, 357–375.

Hocking, L. 1963 The instability of a non-uniform vortex sheet. *J. Fluid Mech.* **18**, 177–186.

Ince, E. L. 1956 *Ordinary Differential Equations.* Dover.

Kelly, R. E. 1967 On the instability of an inviscid shear layer which is periodic in space and time. *J. Fluid Mech.* **27**, 657–689.

Lasheras, J. C. & Choi, H. 1988 Three dimensional instability of a plane free shear layer: an experimental study of the formation and evolution of the streamwise vortices. *J. Fluid Mech.* **189**, 53–86.

Maslowe, S. E. 1986 Critical layers in shear flows. *Ann. Rev. Fluid Mech.* **18**, 405–432.

Michalke, A. 1964 On the inviscid instability of the hyperbolic tangent profile. *J. Fluid Mech.* **19**, 543–556.

Moser, R. D. & Rogers, M. M. 1993 The three dimensional evolution of a plane mixing layer. *J. Fluid Mech.* **247**, 275–320.

Nygaard, K. J. & Glezer, A. 1991 Evolution of streamwise vortices and generation of small scale motion in a plane mixing layer. *J. Fluid Mech.* **231**, 257–301.

Pierrehumbert, R. T. & Widnall, S. E. 1982 The two- and three-dimensional instabilities of a spatially periodic shear layer. *J. Fluid Mech.* **114**, 59–82.

Rayleigh, Lord 1880 On the stability and instability of certain fluid motions. *Proc. Lond. Math. Soc.* **11**, 57–70.

Wundrow, D. W. 1996 Linear instability of a uni-directional transversely sheared mean flow. *NASA Contractor Rep.* 198535, October.

Wundrow, D. W. & Goldstein, M. E. 1994 Nonlinear instability of a unidirectional transversely sheared mean flow. *NASA Tech. Mem.* 106779.

Zaman, K. B. M. Q. 1993 Streamwise vorticity generation and mixing enhancement in free-jets by Delta-tabs. *AIAA Paper* 93-3253.